DEPARTMENT OF DEFENCE
DEFENCE SCIENCE & TECHNOLOGY ORGANISATION
DSTO

DSTO

A Parametric Analysis of a Coupled Chemistry-Radiation Model in Porous Media

Farid C. Christo

DSTO-RR-0188

DISTRIBUTION STATEMENT A
Approved for Public Release
Distribution Unlimited

20010406 087

A Parametric Analysis of a Coupled Chemistry-Radiation Model in Porous Media

Farid C. Christo

Weapons Systems Division
Aeronautical and Maritime Research Laboratory

DSTO-RR-0188

ABSTRACT

A one-dimensional coupled chemistry-radiation model (ChemRad) for predicting combustion and heat transfer characteristics in a single and multi-layered porous media is presented. The model allows detailed gas and surface chemical kinetics mechanisms to be incorporated, and uses a two-flux radiation approximation in the energy equation. A stoichiometric propane/air mixture burning in a thin wire-mesh burner has been modelled using a well-documented high-temperature propane kinetics scheme with 40 reactive species and 93 reactions. A systematic analysis of the solution's sensitivity to variations in input parameters, particularly the optical characteristics of the media, has been performed and influential parameters have been identified. It has been found that the dominant factors that influence the solution, in order of significance are the area density, voidage and reflectivity of the porous material, and the ratio of forward-to-backward scattering of radiation.

RELEASE LIMITATION

Approved for public release

DEPARTMENT OF DEFENCE
DEFENCE SCIENCE & TECHNOLOGY ORGANISATION
DSTO

AQ F01-07-1141

Published by

DSTO Aeronautical and Maritime Research Laboratory
PO Box 4331
Melbourne Victoria 3001 Australia

Telephone: (03) 9626 7000
Fax: (03) 9626 7999
© Commonwealth of Australia 2000
AR-011-608
October 2000

APPROVED FOR PUBLIC RELEASE

A Parametric Analysis of a Coupled Chemistry-Radiation Model in Porous Media

Executive Summary

The accuracy and reliability of numerical models to predict combustion and thermal radiation characteristics of gaseous and solid fuels, relies heavily on their ability to adequately couple the various transport mechanisms in the process. These processes usually include chemical reactions, turbulent mixing, and radiation heat transfer. The work presented here is aimed at developing a numerical model (*ChemRad*) to calculate the laminar combustion inside porous media, accounting for detailed chemistry and radiative heat transfer. This study is part of an ongoing research program aiming at developing computational capabilities to model the performance of infrared (IR) emitting devices. More specifically to assess the potential use of porous radiant burner technologies in the design of a new generation of IR tracking and decoy devices.

The numerical model presented here has a unique capability for handling complex and detailed chemical kinetics accurately and efficiently, hence eliminating chemistry-related errors in the solution. The greatest source of errors in the model, however remains the uncertainty in some input parameters that describe the microstructure and optical properties of the porous medium. Accordingly a systematic analysis of the solution's sensitivity (or lack of it) to variations in nine input parameters has been conducted. Three of the parameters; voidage, tortuosity, and area density represent the microstructural properties of the porous medium, and the remaining six parameters describe the optical properties of the porous material. These are the emissivity, reflectivity, single scattering albedo, extinction coefficient, forward- and backward radiation scattering fractions. It has been found that the most influential parameters (in order of significance) are the area density, voidage, reflectivity, and the forward-to-backward scattering ratio.

The capability of the *ChemRad* model to capture the combustion characteristics has been successfully demonstrated by a favourable agreement between the model predictions and the experimental results, which are documented in a separate technical report to be published soon.

Author

Farid C. Christo
Weapons Systems Division

Farid Christo completed his B.Sc.(1986) and M.Sc. (1989) in Aeronautical Engineering at the TECHNION-I.I.T, followed by one year working as a research engineer at the Technion-R&D Institute. In his undergraduate studies he majored in thermo-fluids and propulsion systems. Farid's M.Sc. research was on experimental investigation of multiphase flows at low Reynolds numbers.

Between 1990 and 1993 he worked at the University of Sydney on a joint project with Pacific Power Corporation. His work focused on the development and validation of computer models to predict the flow field and erosion rate of heat recovery tubes inside the boilers of coal-fired power stations.

Between 1993-1996, he undertook Ph.D. research at the University of Sydney, Department of Mechanical and Mechatronic Engineering. His research topic was the development of artificial neural networks for applications in turbulent combustion simulations. Upon completion of his doctorate Farid joined the Sydney-based company Biomass Energy Services and Technology, where he worked on modelling industrial aerodynamics and combustion processes. In April 1998 he joined the DSTO as a Research Scientist with Weapons Systems Division, Salisbury.

Farid's current research objective is to develop advanced computational capabilities for modelling the aerothermochemical and radiative fields of generic pyrotechnic compositions. This work will provide DSTO with the capability to evaluate the performance of new and existing pyrotechnic formulations with minimal dependence on complex and expensive experimental procedures.

Contents

1. Introduction

During the last decade the utilisation of Porous Radiant Burner (PRB) technology has emerged as a practical method for developing combustion systems with low hazardous emissions gases, such as CO and NO_x [1-3]. Another advantage of a PRB is its capability to maintain stable combustion of premixed flame and enhanced radiation heat transfer over a wider operating range than a conventional "blue-flame" premixed burner [4]. PRB technologies have been primarily driven by the need to improve the thermal efficiency of existing heat and power generating facilities and also by the restrictions on the emission levels of hazardous gases. To the best knowledge of the author no published research exist that attempts to examine the potential use of PRB technology for Defence applications, for example as Infrared (IR) decoys or tracking devices. The "Hot Brick" technology uses a similar concept to the PRB, but it electrically heats a solid block of metal to a high temperature causing it to emit in the IR wave band. It is anticipated that the present work will deliver numerical capability that will assist in determining the suitability of PRB technology for applications as IR emitting devices.

The objectives of this study are firstly to develop a numerical model to simulate the combustion process in porous media accounting for coupled chemistry-radiation processes. Secondly to perform a sensitivity analysis of the model's parameters, particularly those that are difficult to accurately determine experimentally or analytically. The capability and robustness of the model will be verified with measurements taken from an experimental PRB. This however is reported in a separate document [5]. This work was conducted as part of an AIR sponsored task, AIR 97/250 "Modelling IR Countermeasures for RAAF".

2. PRB Concept

Porous radiant burners are manufactured either from ceramic or stainless steel fibers or from fired clay. Approximately 90 to 95 percent of the porous medium consist of micro pores. The porous medium being typically at around 900 degrees centigrade radiates energy and depending on the emissivity of the material, heat flux intensity of more than 300kW per square meter can be achieved. In principle, the combustion process in a PRB is a premixed-based combustion but with a fundamental difference from a "blue-flame" burner in the mechanism in which heat is transferred. Unlike conventional premixed flame, shown schematically in Fig.1 (top), in which heat convection is the dominant mode of heat transfer, PRB transfers heat mainly by thermal radiation as illustrated in Fig.1 (bottom). Close-up photographs of blue- and porous-burner flames are shown in Fig. 2, and clearly explain the origin of the term 'blue flame'.

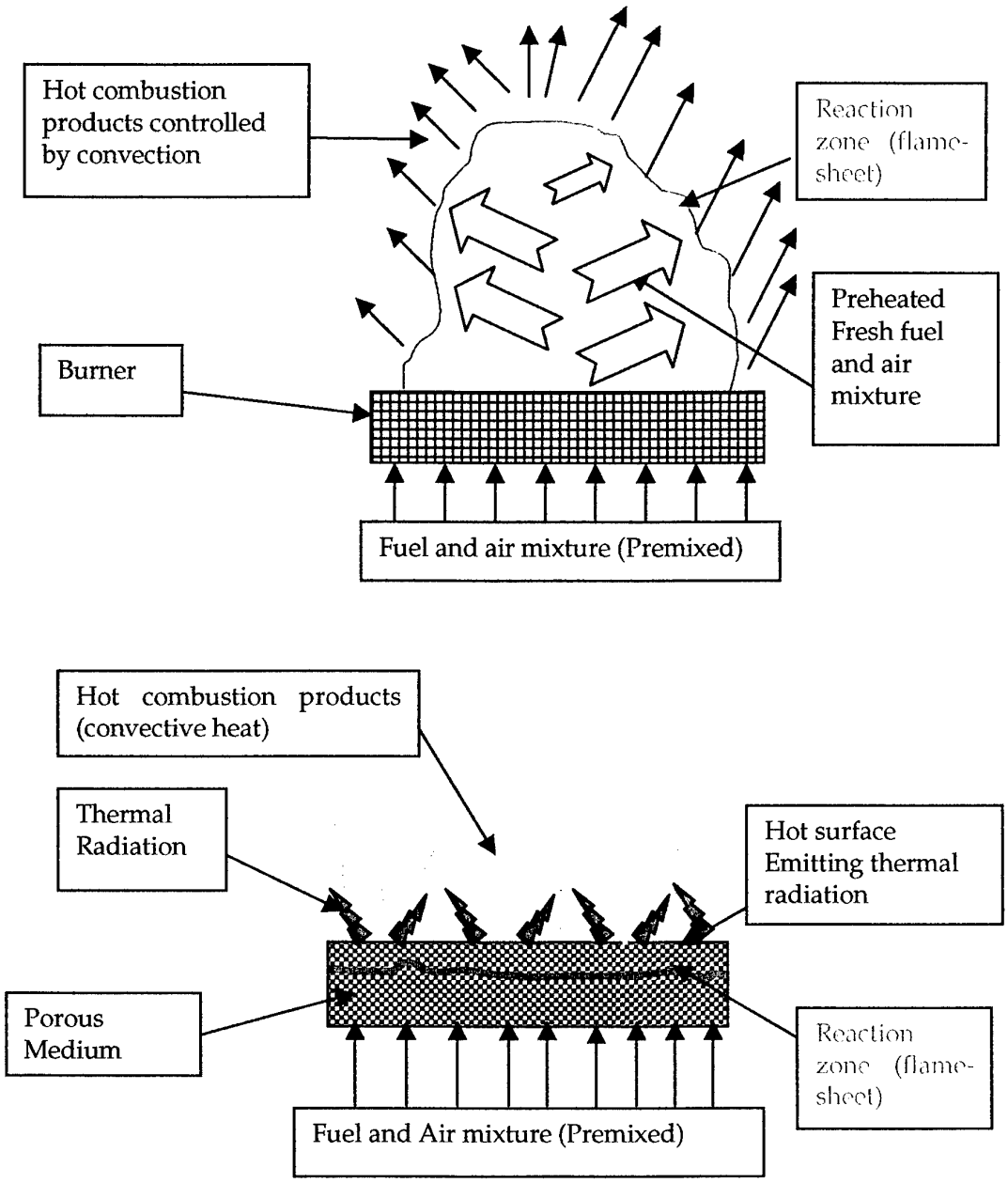

Figure 1: Schematic Illustrations of 'blue flame' (top) and porous radiant flame (bottom).

In PRBs some of the radiant heat is also recirculated to the unburnt mixture. Such recirculation of heat without simultaneous dilution by the burnt gases has the effect of extending the flammability limits and improving flame stability [6-8]. The heat transfer from the reaction zone inside the porous medium to the solids causes the solids to

radiate thus lowering the flame temperature and consequently reducing (thermal) NO_x emissions.

The improved characteristics of PRB combustion include increasing the flame speed, decreasing the lean flammability limit and enabling the burning of low heat-content fuels. A number of studies [9,10] showed that CO is created and "consumed" (converted into CO_2) within the porous medium. They also showed those important radicals such as OH, H and O, peak within the porous layer and almost all NO formation occurs within the porous medium because the gas temperature loses enough heat to the solids to suppress the thermal NO_x reactions. To illustrate the effect of thermal radiation on the combustion temperature, a comparison of gas temperature in a porous burner and a conventional burner-stabilised blue flame is shown in Fig. 3. These calculations are carried out using the *ChemRad* model, which will be described in a later section, and refer to a stoichiometric propane/air mixture and identical inlet conditions (*e.g.* reactants composition, temperature, flow rate etc.) for both burners. It is clear from the figure that the flame temperature in a porous burner is lower than that in a 'blue-flame' burner by approximately 700K. This difference is primarily attributed to the enhanced radiative heat transfer of the porous burner.

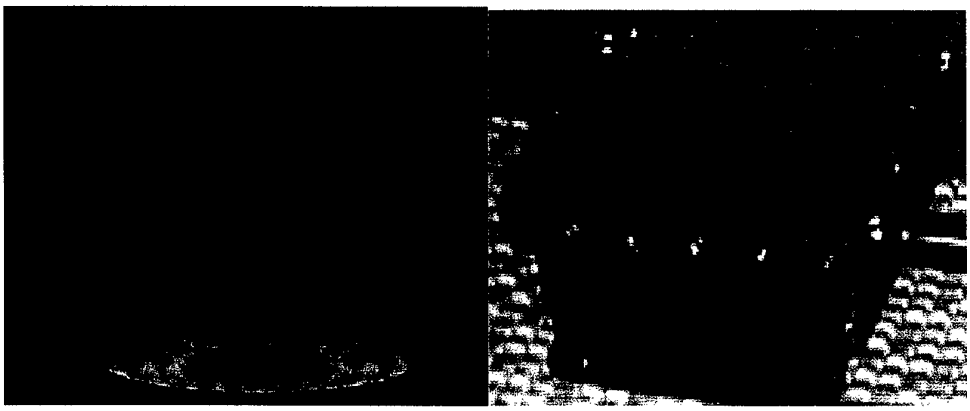

Figure 2. A close-up photograph of Sydney University's "Blue Flame" burner (left) and DSTO's Porous Radiant Burner (right).

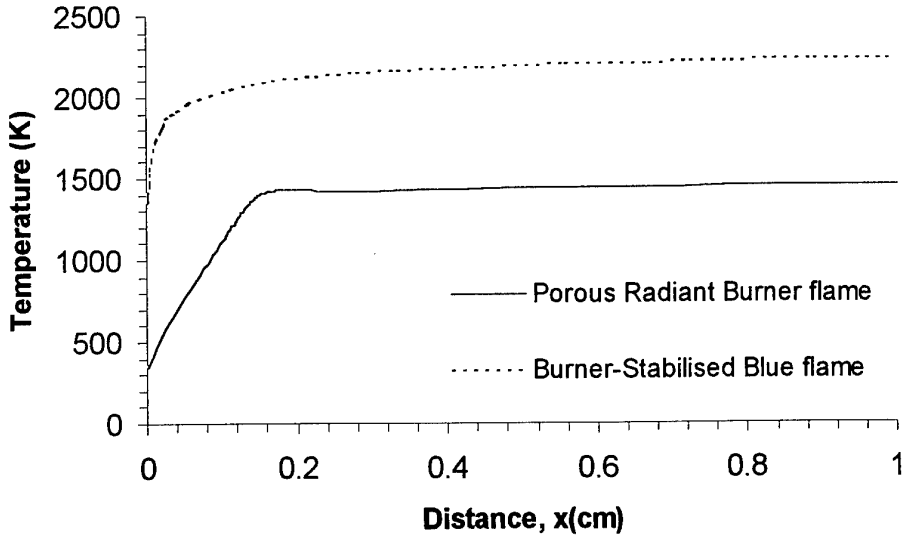

Figure 3: *A comparison between the adiabatic gas temperature in a porous burner and that in a burner-stabilised blue flame, for a stoichiometric propane/air mixture.*

3. The Numerical Model

The numerical model is one-dimensional, laminar, adiabatic model. It includes a separate energy equation for the gas and the solid-phase accounting for conduction, convection, and radiation heat transfer mechanisms in all phases. The model allows detailed chemistry of gaseous species and surface reactions to be incorporated.

3.1 Model Description

The coupled chemistry-radiation model *ChemRad,* is capable of handling a single or multi-layered burner of different porous media and applies for planar, cylindrical or spherical geometry. The *ChemRad* model is based on the work of Shardlow[11], and utilises the core routines of the chemical kinetics package, CHEMKIN [12-15]. In the present study the porous medium has been represented as a thin three-layered mesh of the same material. The geometry and material used in the model have been selected to match those of an experimental PRB, which has been investigated in a separate study [5]. A schematic description of the model is shown in Fig. 4.

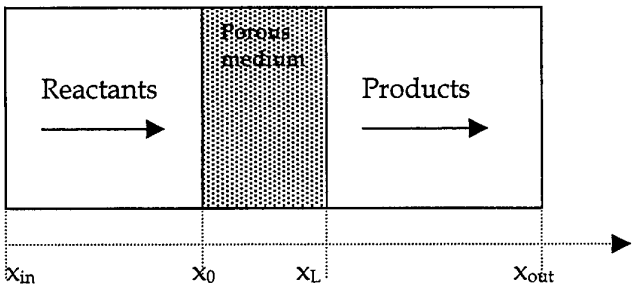

Figure 4: Schematic description of the computational domain for the porous burner model.

Users are required to specify the reactants compositions, inlet temperature, burner (computational) dimensions, and the physical and optical properties of the porous material.

3.2 Governing Equations

The governing equations for mass, species, and energy conservation are described next. In these equations, ρ is the gas density, u is the gas velocity, ϕ is the porosity of the solid (ϕ=1 in the gas region), Y_k, V_k, W_k and ω_k are the mass fraction, diffusive velocity, molecular weight, and the production rate of the *kth* species, respectively. It should be mentioned here that the governing equations presented below do not include the surface reactions terms, which have not been accounted for in this study. A comprehensive description of the governing equations, including the terms for surface chemistry can be found in Ref.[11].

3.2.1 mass continuity equation

$$m'' = \rho u \phi , \tag{1}$$

where m'', is the mass flow rate per unit area.

3.2.2 gas species conservation equation

$$\rho u \phi \frac{dY_k}{dx} + \frac{d}{dx}\left(\rho u Y_k V_k\right) = \omega_k \, W_k \phi \ldots k = 1, kk \tag{2}$$

where kk, is the total number of gaseous species.

3.2.3 gas-phase energy equation

$$\rho u \phi c_{pg} \frac{dT_g}{dx} - \frac{d}{dx}\left(k_{g,e} \frac{dT_g}{dx}\right) + \sum_{k=1}^{kk} \rho \phi Y_k V_k c_{pg} \frac{dT_g}{dx} + h_v (T_g - T_s) = -\sum_{k=1}^{kk} \omega_k \; h_k W_k \phi \,, \quad (3)$$

where c_{pg} is the specific heat of the *kth* gaseous species, T_g , T_s are the gas and solid temperatures, respectively, h_v is the volumetric heat transfer coefficient, h_k is the enthalpy of the *kth* species and $k_{g,e}$ is the effective thermal conductivity of the gas ($\approx \phi k_g$).

The production rate term (ω_k) is calculated using the kinetic mechanism that describes the chemistry of the fuel . A general form for representing the chemistry of kk^{th} chemical species is:

$$\sum_{k=1}^{kk} \upsilon_{ki}^{'} \Lambda_k \Leftrightarrow \sum_{k=1}^{kk} \upsilon_{ki}^{''} \Lambda_k \cdots (i = 1,...,I) \,, \quad (4)$$

where ν_{ki} are the stoichiometric coefficients, I is the total number of reactions, and Λ_k is the chemical symbol of the *kth* species. The superscripts ` and `` refer to the forward and backward stoichiometric coefficients, respectively. Accordingly, the term for the production rate for the set of chemical reactions described by Eq. (4), is given as:

$$\omega_k = \sum_{i=1}^{I} \upsilon_{ki} \left[k_{fi} \prod_{k=1}^{kk} [X_k]^{\upsilon_{ki}^{'}} - k_{bi} \prod_{k=1}^{kk} [X_k]^{\upsilon_{ki}^{''}} \right] \cdots (k = 1,...,kk) \,, \quad (5)$$

where $[X_k]$ is the molar concentration of the *kth* species, and k_{fi} , k_{bi} are the forward and backward rate constants of the *ith* species, respectively. The forward rate constant, k_f is calculated using the Arrhenius temperature dependence formula:

$$k_{fi} = A_i T^{\beta_i} \exp\left(\frac{-E_i}{RT}\right). \quad (6)$$

In Eq. (6) the pre-exponential factor A_i, the temperature exponent β_i , and the activation energy E_i , are specified by the kinetic mechanism. The backward rate constant k_{bi}, is calculated indirectly from the equilibrium rate constant k_{ei}:

$$k_{bi} = \frac{k_{fi}}{k_{ei}}, \quad (7)$$

where the equilibrium constants k_{ei} is given by:

$$\ln(k_{ei}) = \sum_{i=1}^{I} (\upsilon_{ki}^{'} - \upsilon_{ki}^{''}) \Delta G^{*}_{ki} - (\upsilon_{ki}^{'} - \upsilon_{ki}^{''}) \ln(\frac{P}{RT}) \,. \quad (8)$$

The Gibbs free energy ΔG_{ki}^* (normalised by RT, R being the universal gas constant) is calculated from the changes in the system's normalised enthalpy ΔH_{ki}^* ,and entropy ΔS_{ki}^*. These terms are correlated in the relationship:

$$\Delta G^*_{ki} = \Delta H^*_{ki} - T\Delta S^*_{ki}. \tag{9}$$

The normalised enthalpy and entropy terms are calculated using the polynomial formulation:

$$\Delta H^*_{ki} = \sum_{n=1}^{N} \frac{a_{nk} T_k^{(n-1)}}{n} + \frac{a_{N+1,k}}{T_k} \tag{10}$$

$$\Delta S^*_{ki} = \sum_{n=2}^{N} \frac{a_{nk} T_k^{(n-1)}}{(n-1)} + a_{1k} \ln(T_k) + a_{N+2,k} \tag{11}$$

where the polynomial coefficients, a_n, are obtainable from a number of databases [16-18].

3.2.4 solid-phase energy equation

$$\frac{d}{dx}\left[k_{e,s}\frac{dT_s}{dx}\right] + h_v(T_g - T_s) = \frac{dq_r}{dx} \tag{12}$$

The terms in Eq. (12) represent conduction, convection and radiation heat transfer, respectively. An empirical correlation has been used to determine the convective heat transfer coefficient h_v , for the porous medium. In the current model of a metal fibre matrix, the Nusselt number has been estimated using the following correlation[19]:

$$Nu_d = 0.10\,\mathrm{Re}_d^{\,1.64}, \tag{13}$$

where the Nusselt and Reynolds numbers are calculated based on the average fibre diameter and room temperature. The effective thermal conductivity of the solid $k_{e,s}$ is evaluated by the following correlation [11]:

$$\frac{k_{e,s}}{k_s} = 1 + \frac{\phi}{[(1-\phi)/m] + [k_s/(k_g - k_s)]}, \tag{14}$$

where the parameter m, is given by:

$$m = \left[1.20 - 29\frac{d}{L_f}\right](0.81-\phi)^2 + \left[1.09 + 2.5\frac{d}{L_f}\right]. \tag{15}$$

In Eq. (15), d and L_f, are the diameter and the length of the fibre.

3.3 Radiation Model

A two-flux radiation model, also known as the Schuster-Schwarzchild approximation has been used to calculate the net radiative flux q_r, in Eq. (12). The model is valid for radiative transfer in absorbing, emitting and scattering media. The main limiting assumption of the model is that the medium properties are such as to yield homogenous absorbing, emitting and scattering of electromagnetic radiation in a forward scattering hemisphere and in a backward scattering hemisphere, separately.

The net radiative flux q_r, is calculated as the difference between the forward radiation flux q^+, and the backward radiation flux q^-, ($q_r = q^+ - q^-$). These radiative transfer fluxes are obtained by solving the following equations:

$$\frac{dq^+}{dx} = -2\sigma_e q^+ + 2\sigma_e \omega_0 (fq^+ + bq^-) + 2\sigma_e (1-\omega_0)\sigma T_s^4 \qquad (16)$$

and,

$$-\frac{dq^-}{dx} = -2\sigma_e q^- + 2\sigma_e \omega_0 (fq^- + bq^+) + 2\sigma_e (1-\omega_0)\sigma T_s^4 . \qquad (17)$$

Here ω_0 is the single scattering albedo, which represents the fraction of attenuated energy that is the result of scattering. For a non-scattering medium $\omega_0=0$, while for pure scattering $\omega_0 = 1$. σ_e , is the extinction coefficient, which represents the fraction of attenuated energy that is the result of absorption and scattering, and f & b are the forward- and backward-radiation scattering fractions, respectively. σ, is the Stefan-Boltzmann constant.

3.4 Boundary Conditions

The boundary conditions required for solving the governing equations consist of user specified inlet conditions and a set of conditions dictated from energy balance considerations. At the inlet ($x=x_{in}$) the gas temperature and the mass fraction of the reactants are known quantities: $T_g=T_{g,in}$, $Y_k=Y_{k,in}$. The boundary condition at the upstream surface of the porous layer $x=x_0$,is established from an energy balance equation:

$$-(1-\phi)k_s \frac{dT_s}{dx}\Big|_{x=x_0} = (1-\phi)h_0 (T_g - T_s) - [q^-(x_0) - q^+(x_0)], \qquad (18)$$

where h_0, is the convective heat transfer coefficient per unit area and k_s, is the thermal conductivity of the solid. The radiative heat transfer components are calculated using:

$$q^+(x_0) = \varepsilon\sigma T_-^4 + \chi_0 q^-(x_0) \tag{19}$$

where T_- is the upstream temperature of the environment to which the upstream boundary of the porous medium is exposed, *i.e.* burner housing. χ_0 ,is the reflectivity of the porous medium, and ε, is the average emissivity of the burner surface. $q^-(x_0)$ in Eq. (17) is the backward radiation fraction at x_0.

The boundary condition at the downstream surface of the burner ($x=x_L$) :

$$q^-(x_L) = \varepsilon\sigma T_+^4 + \chi_0 q^+(x_L), \tag{20}$$

T_+ being the downstream temperature of the environment to which the downstream boundary of the porous medium is exposed *i.e.* the ambient temperature. At the outlet $x=x_{out}$, the boundary conditions are $dT_g/dx=0$ and $dY_k/dx=0$. These conditions imply that the chemical reactions are completed and the process is adiabatic.

3.5 Numerical Solver

The method for solving Eqs. 1-20, is to discretise the conservation equations establishing a set of simultaneous algebraic equations that are applied on discrete mesh points within a predetermined computational domain. The core solver is based on Sandia's PREMIX module[14], and makes use of the well-known CHEMKIN package[12-15]. It uses a combined time-dependent and steady state method. That is, a modified damped Newton method is initially used to solve the non-linear algebraic equations by an iterative process. If the Newton method fails to achieve the required level of convergence, then a time-stepping algorithm is used. The idea is to determine the steady-state solution by solving transient equations, namely for each of the conservation equations (mass, species, etc..) an additional time-dependent component is added. For example, an extra term dY_k/dt is added in the left-hand side of Eq. 2. The combination of Newton and time-stepping methods utilises the advantage of the rapid convergence of Newton's method, and the robustness of the time-stepping algorithm for handling the stiffness problem.

An adaptive meshing placement is a powerful tool to alleviate convergence difficulty and reduce the user intervention in influencing the convergence of the solution. The iterative process commences with a coarse mesh, which is easy to converge and provides an improved guess over that specified by the user. The refinement of mesh is then done automatically allowing more mesh points to be inserted in regions with high gradients and/or curvatures in the concentration profiles. The gradient (GRAD) and curvature (CURV) parameters have a strong effect on the convergence rate (but not on

the solution's accuracy). The parameter GRAD determines the number of additional mesh point to be inserted in regions with high gradients of concentrations, while CURV controls the number of additional points to be added in regions with high curvature in the concentration profiles. Lower numbers for GRAD and CURV mean more mesh points will be inserted each time the adaptive mesh routine is called. The default values for GRAD and CURV are 0.1 and 0.5, respectively. However, it has been found that in some cases a GRAD value of 0.1 could be too restrictive for achieving a fully converged solution. This is especially true near a flame front where sharp changes in radicals' concentration create large gradients and curvatures in concentration profiles of radical species. Furthermore, inserting more mesh points does not necessarily improve the accuracy of the solution, but it definitely demands more computing resources. Since Newton algorithm is more likely to converge on a coarse mesh, the strategy used was to start the computations with a coarse grid and relaxing the GRAD parameter, to say 0.8. Once a solution has been achieved the value of GRAD is then reduced and the computations are repeated restarting from the previously converged solution. This cycle is continued until the required accuracy is achieved. Typically, GRAD and CURV values of 0.3 and 0.5, respectively, have been used.

Convergence of the solution is achieved when the residuals of the discretised conservation equations for mass and energy are reduced to a pre-selected tolerance and when the mesh is sufficiently refined to meet specified gradient and curvature criteria of the solution profiles. Details on the numerical schemes, the adaptive mesh algorithm and convergence criteria can be found in Refs[12-15].

4. Model Parameters

A schematic block diagram of the structure of the code is given in Fig. 5. The numerical model requires a number of input parameters that include gas phase kinetics and optionally surface reactions, thermodynamic and transport properties of all species in the reactions mechanism. Also required are the physical and optical properties of the porous medium.

4.1 Chemical Kinetics Model

All simulations have been carried out for a stoichiometric propane/air mixture. The chemistry of propane (C_3H_8) has been represented by a kinetics mechanism with 40 reactive species and consists of 93 elementary reactions. The kinetic scheme included also NO_x formation and reburning kinetics that have been adopted from the GRI 2.1 mechanism[20]. The details of the propane mechanism are given in Appendix A.

4.2 Numerical Parameters and Physical Properties

The model-input parameters include burner geometry, firing rate, and reactants' mole fractions. The porous medium is represented in the model as a single layer, 3mm in thickness made of INCONEL601 fibre matrix of 0.4mm wires. INCONEL601 is a nickel-chromium alloy (typical composition is 80% Ni, 16% Cr, and 4% Fe) which is used in many engineering applications. It has excellent mechanical properties and is resistant towards oxidation in air for up 1093 °C. The total hemispheric emissivity ε, of INCONEL601 varies modestly with temperature. For example at a temperature of 315°C, the emissivity ε is 0.69, but it increases to 0.82 at 980°C. Since the operating temperature of the PRB is expected to be in a temperature range around 900°C, a representative emissivity value of 0.8 has been selected and used in all calculations.

For simplicity the computational domain used in this study starts at the upstream edge of the porous medium , ie. $x_{in}=x_0=0$, and extends to $x_{out}=10\ mm$ in the downstream direction, see Fig. 3. The physical and optical properties of the porous medium such as thermal conductivity, emissivity and so forth, are also required. Table 1 summarises the input parameters that have been used and kept unchanged in all the calculations. The values of these parameters are selected to closely represent those of the experiment so a consistent comparison can be made.

Table 1: List of parameters that have been kept unchanged throughout all the calculations.

Property (units)	Value
Propane mole fraction (-)	0.042
Equivalence ratio (-)	1.0
Firing rate (kW/m^2)	417.
Mixture's inlet temperature (K)	350
Thermal conductivity of mesh (W/m.K)	27.5
Wire-mesh thickness (mm)	0.4
Porous medium thickness (mm)	3.0
Computational domain length (mm)	10

4.3 Sensitivity Analysis

To examine the effect of variations (due to uncertainty) in some input values on the solution, a systematic sensitivity analysis has been carried out. The gas and solid temperatures, concentration profiles of CO, CO_2, OH, and the net radiation flux have been selected as indicators to determine the solution's sensitivity (or lack of it) to variations in any specific input parameter. Sensitivity analysis has been performed against a total of nine input parameters: three parameters that describe the porous medium property and structure, namely voidage, tortuosity, and area density, and six

parameters that describe the optical properties of the medium. These are the emissivity, reflectivity, single scattering albedo, extinction coefficient, and the forward- and backward-scattering fractions. A list of the various input configurations that have been examined is shown in Table 2. The approach used for selecting the optical parameters shown in Table 2, is first to examine the solution's sensitivity at the extreme limits of a certain parameter, *e.g.* for the single scattering albedo (ω_o) such limits are 0.1 and 0.9. Then the sensitivity analysis is repeated for a value that closely reflects the actual property of the porous material that is used in the experiment. For example a single scattering albedo of 0.7 is typical for many Nickel based materials.

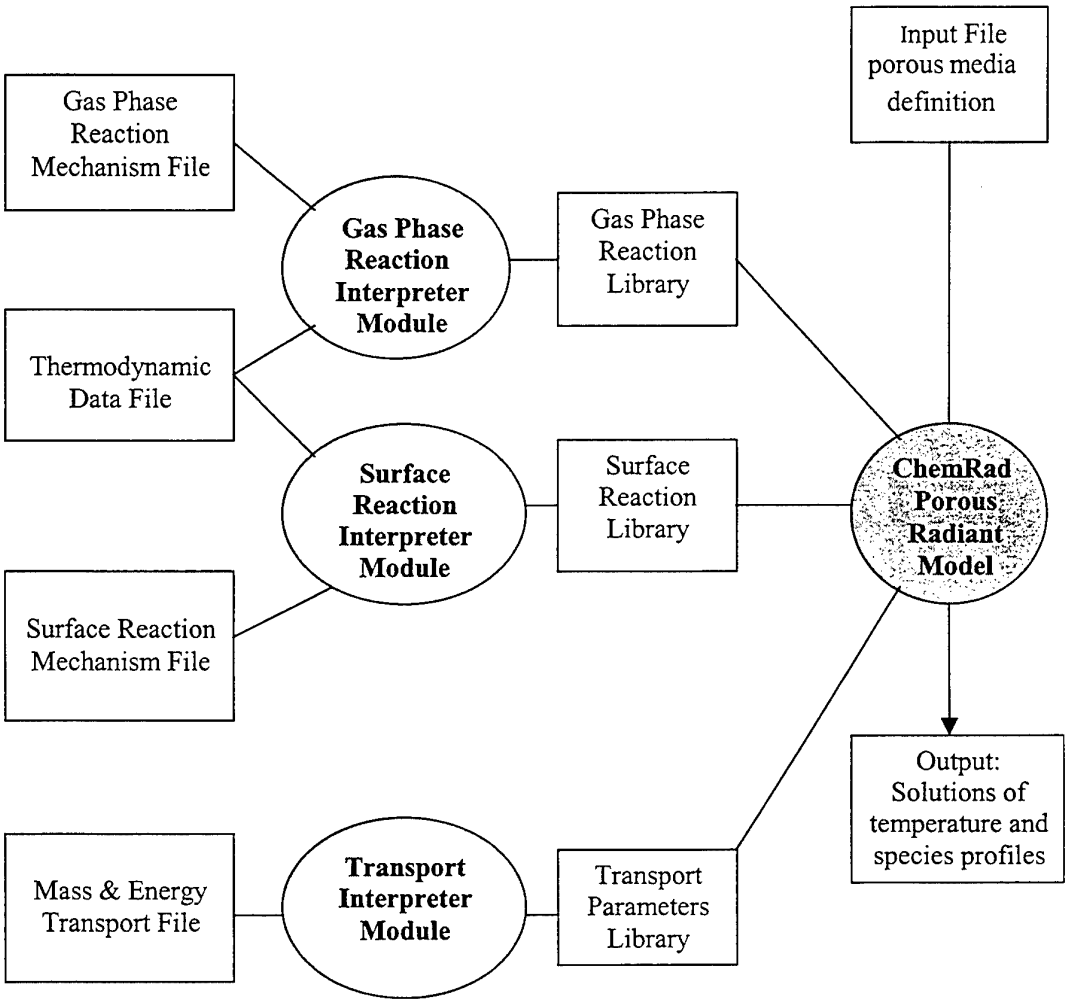

Figure 5: A block diagram of the structure of the ChemRad porous burner model.

Table 2: Summary of the various configurations that have been examined.
Key: ϕ = Void, γ = Tortuosity, A_{den}= Area Density(cm^2/cm^3), ε = Emissivity, χ_0 = Reflectivity, ω_0= Single Scattering Albedo, σ_e= Extinction coefficient(cm^{-1}), f & b = forward- and backward-radiation scattering fractions, respectively.

Configuration	ϕ	γ	A_{den}	ε	χ_0	ω_0	σ_e	f	b
C1	0.9	1.12	7	0.8	0.6	0.7	50	0.5	0.5
C2	***0.3***	1.12	7	0.8	0.6	0.7	50	0.5	0.5
C3	0.9	1.12	***70***	0.8	0.6	0.7	50	0.5	0.5
C4	0.95	1.12	44	0.8	0.6	0.7	50	0.5	0.5
C5	0.95	1.12	44	0.8	0.6	0.7	***5***	0.5	0.5
C6	0.95	***3.36***	44	0.8	0.6	0.7	5	0.5	0.5
C7	0.95	3.36	44	0.8	0.6	0.7	***50***	0.5	0.5
C8	0.95	3.36	44	0.8	***0.1***	0.7	50	0.5	0.5
C9	0.95	3.36	44	0.8	***0.9***	0.7	50	0.5	0.5
C10	0.95	3.36	44	0.8	0.9	***0.1***	50	0.5	0.5
C11	0.95	3.36	44	0.8	0.9	***0.9***	50	0.5	0.5
C12	0.95	3.36	44	0.8	0.9	0.9	50	***0.1***	***0.9***
C13	0.95	3.36	44	0.8	0.9	0.9	50	***0.8***	***0.2***

5. Results and Discussion

Figures 6-17 show the modelling results that correspond to the configurations listed in Table 2. For cases where the solution does not change beyond a certain point, the results are displayed only over that relevant portion of the computational domain. By simultaneously inspecting the parameters shown in Table 2, and the corresponding figures it is possible to identify the effect of variations in one or more of the parameters on the solution. For example, comparing configurations C1 and C5 allows the combined effect of variation in area density and extinction coefficient to be examined.

By comparing the results of cases C1 and C2, the effect of void can be identified. It is shown that reducing the voidage of the porous medium by a factor of 3 causes an increase in the gas and solid temperatures by 10%, and 6%, respectively. The concentration of CO_2 at the exit plane of the burner (x=0.3 mm) has increased by around 2%. However, CO has increased by 25%, and OH by a factor of 2.4. This is mainly due to the sensitivity and strong dependence of CO and OH concentrations on the flame temperature. The net radiation is also increased (by a factor of 2) as expected because reducing the voidage leads to an increase in the residence time of the combustion gases and the contact surface of solid and gas, hence enhancing heat transfer within the porous layer.

Comparing C1 and C3 shows the effect of an increase in area density. In this case an increase in area density by a factor of ten resulted in a reduction of the gas temperature by approximately 180K, and increased the solid temperature by approximately 270K. However, while concentrations of CO and CO_2 have slightly increased and the OH radicals have slightly reduced, the net radiation flux has increased by a factor of four. This is primarily due to the increase in the surface area between the porous medium and the hot combustion products. This has the effect of enhancing heat transfer from the gas stream to the solid hence lowering the gas temperature and increasing the solid temperature. A high temperature of the solid combined with high emissivity causes an enhanced thermal radiation transfer. The changes in OH and CO_2 concentrations can probably be attributed to the low gas temperature, but the cause for the increase in CO is not fully understood yet.

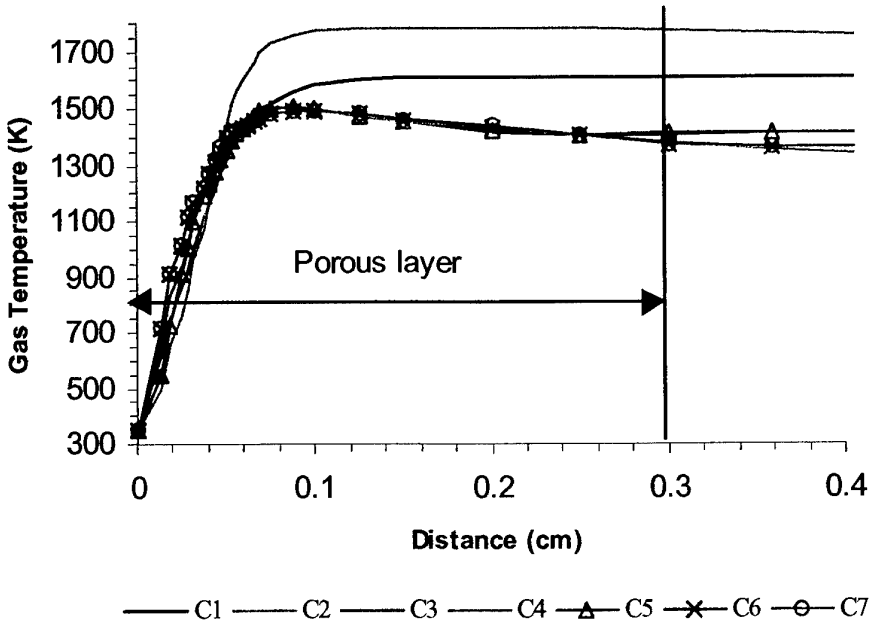

Figure 6: Axial distribution of gas temperature for configurations C1-C7 as listed in Table 2.

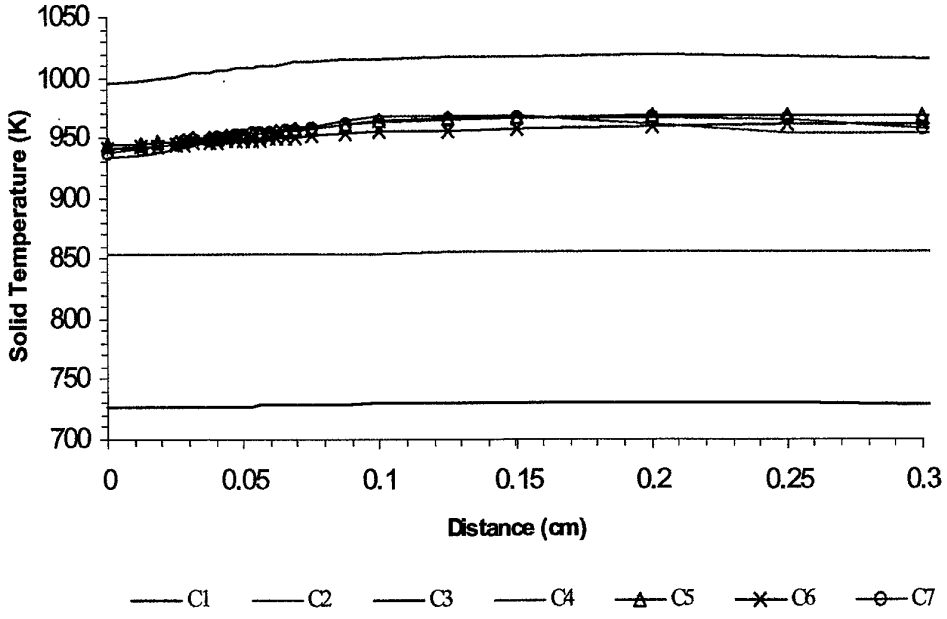

Figure 7: *Axial distribution of solid temperature within the porous medium for configurations C1-C7 as listed in Table 2.*

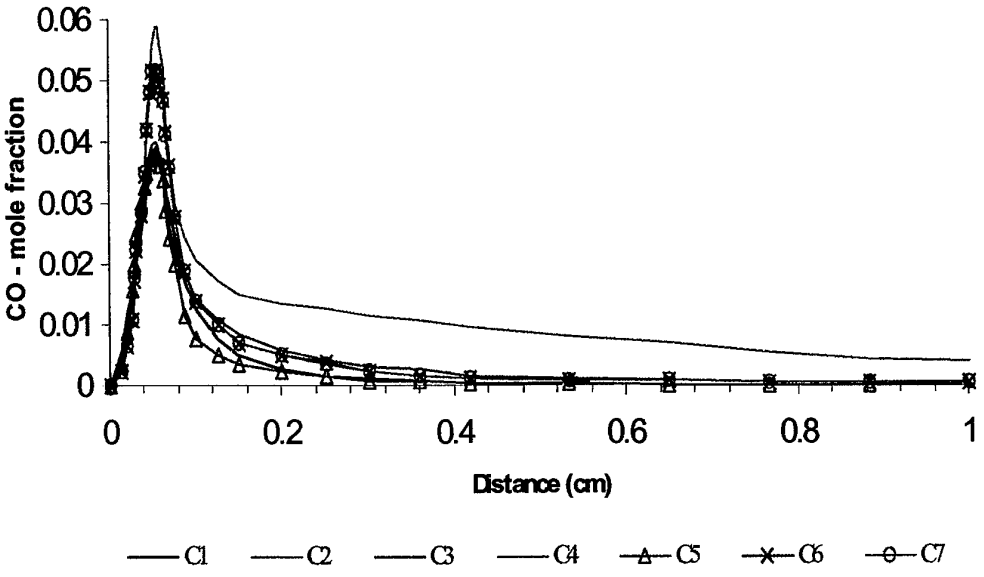

Figure 8: *Mole fraction profiles of CO for configurations C1-C7 as listed in Table 2.*

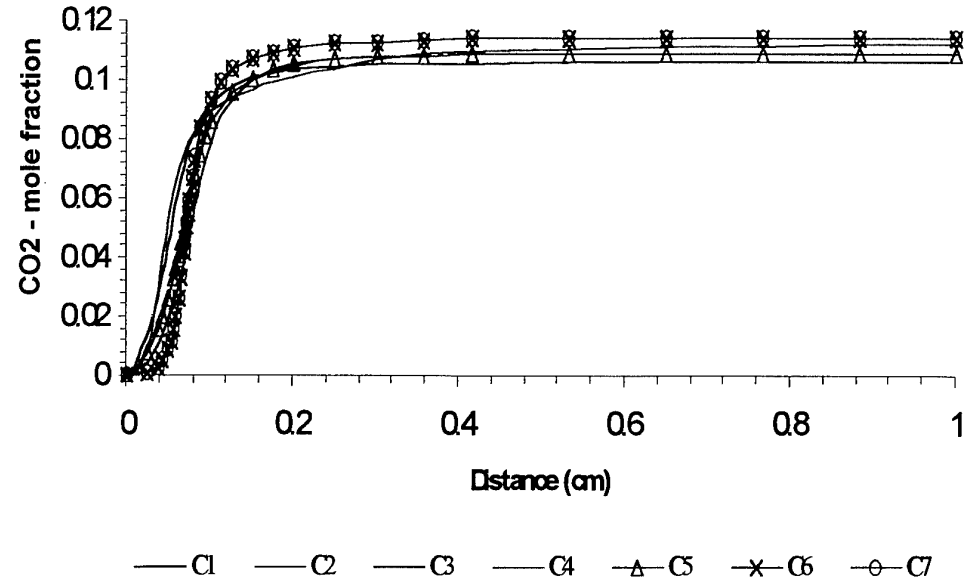

Figure 9: *Mole fraction profiles of CO_2 for configurations C1-C7 as listed in Table 2.*

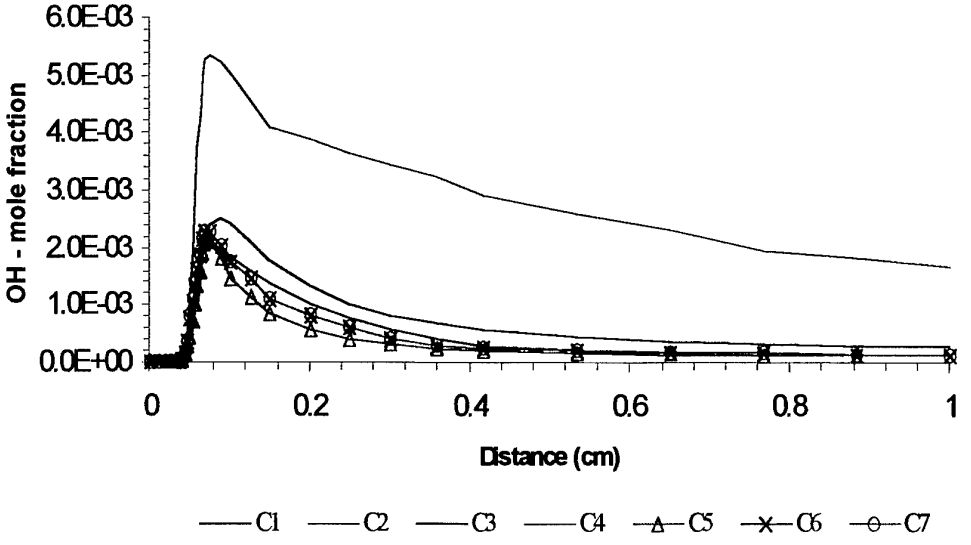

Figure 10: *Mole fraction profiles of OH radicals for configurations C1-C7 as listed in Table 2.*

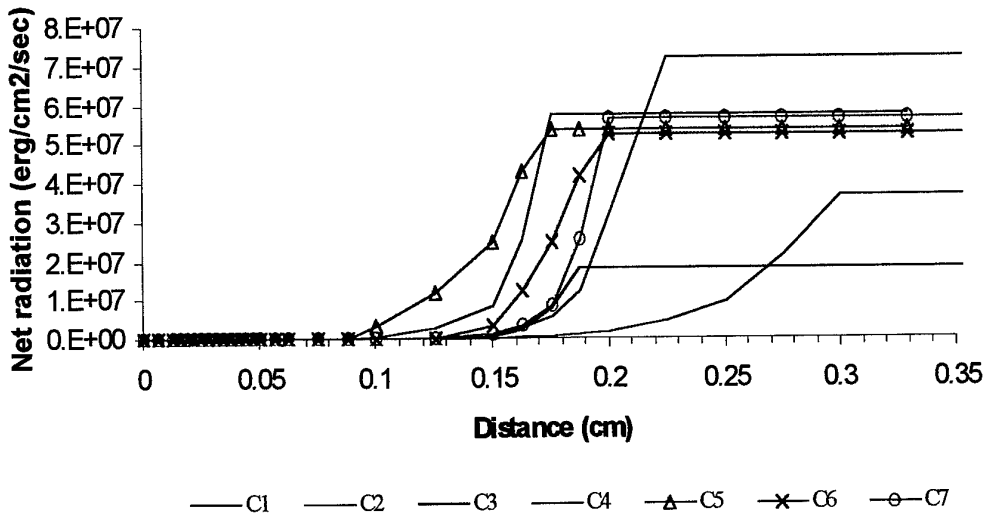

Figure 11: Net radiation for configurations C1-C7 as listed in Table 2.

Configurations C4 and C5 examine the effect of reducing the extinction coefficient by a factor of 10, which interestingly did not record significant effect on the results. In general, however, changes in the extinction coefficient usually have profound effect on the flame stability and combustion characteristics in a thick porous medium with small pore dimensions. This is not the case here therefore the effect of the extinction coefficient is not evident. The only noticeable effect is a small decrease in the net radiation of approximately 5%, as shown in Fig. 11.

The effect of the porous medium tortuosity is examined by comparing configurations C5 and C6. An increase in the tortuosity by a factor of three did not show any significant changes in the temperature or the concentration profiles. Also, the combined effect of changing both the tortuosity and the extinction coefficient (comparing C4 and C6) did not show significant effect on the results.

The effect of variations in reflectivity, scattering albedo and the ratio between the forward and backward scattering fractions, are shown in Figure 12-17. Comparing cases C8 and C9, shows that reducing the reflectivity by a factor of nine, causes a noticeable increase in the gas and solid temperatures by approximately 110K (~8%) and 300K (35%), respectively. The net radiation also increases by a factor of two, however the concentration of CO, CO_2 and OH did not change significantly. These results indicate that heat transfer mechanism by thermal radiation dominates over conduction heat transfer.

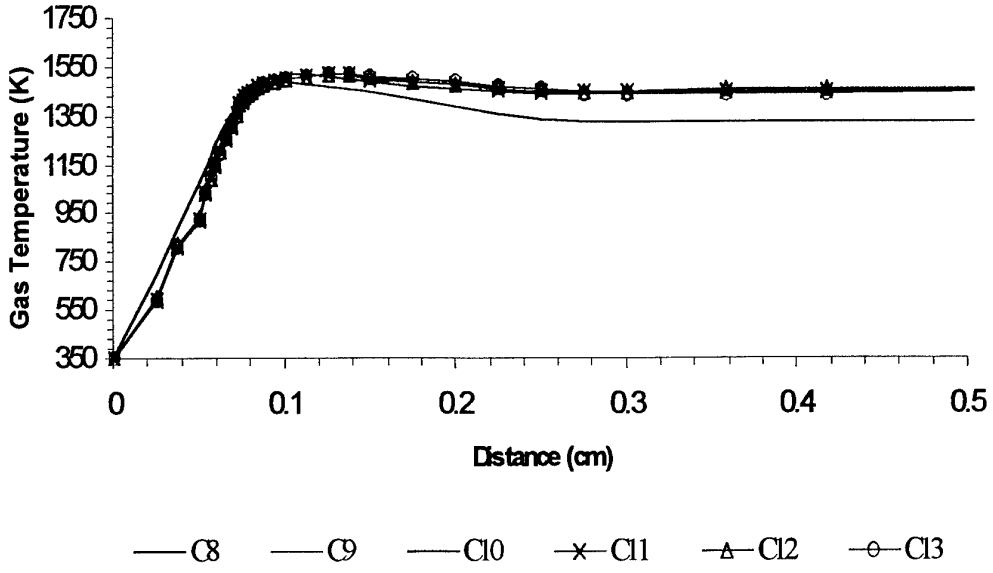

Figure 12: Gas temperature profiles for configurations C8-C13 as listed in Table 2.

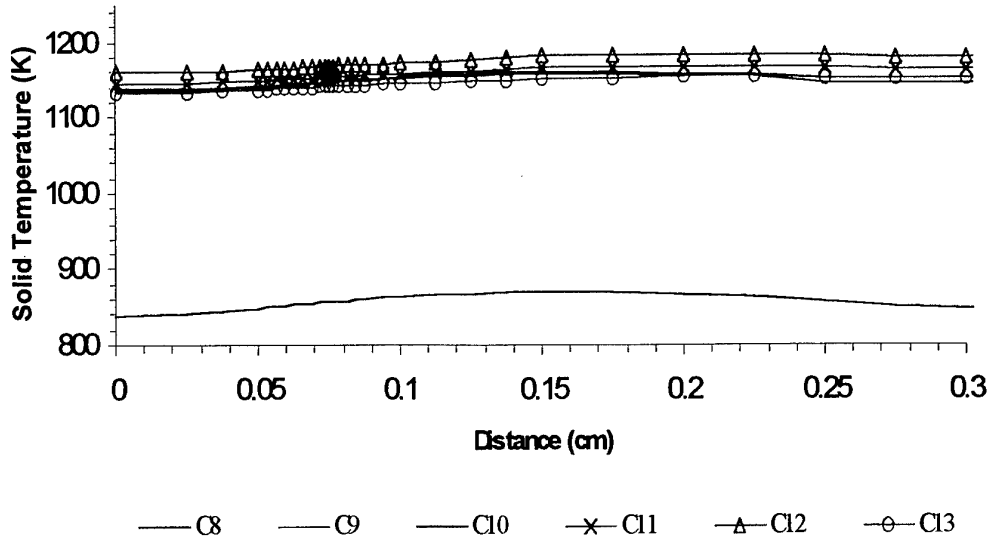

Figure 13: Solid temperature profiles within the porous layer for configurations C8-C13 as listed in Table 2.

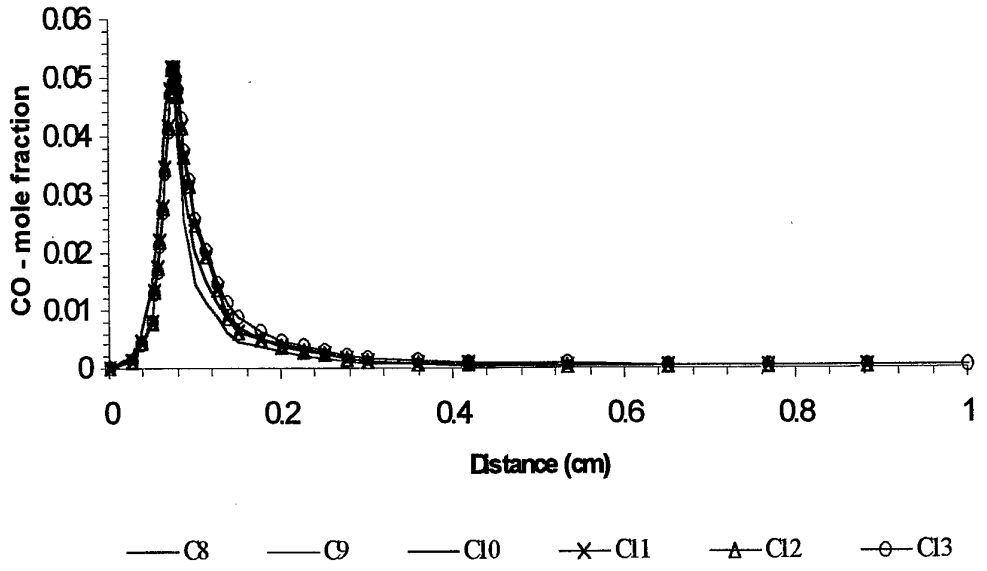

Figure 14: CO mole fraction profiles for configurations C8-1C13 as listed in Tables 2.

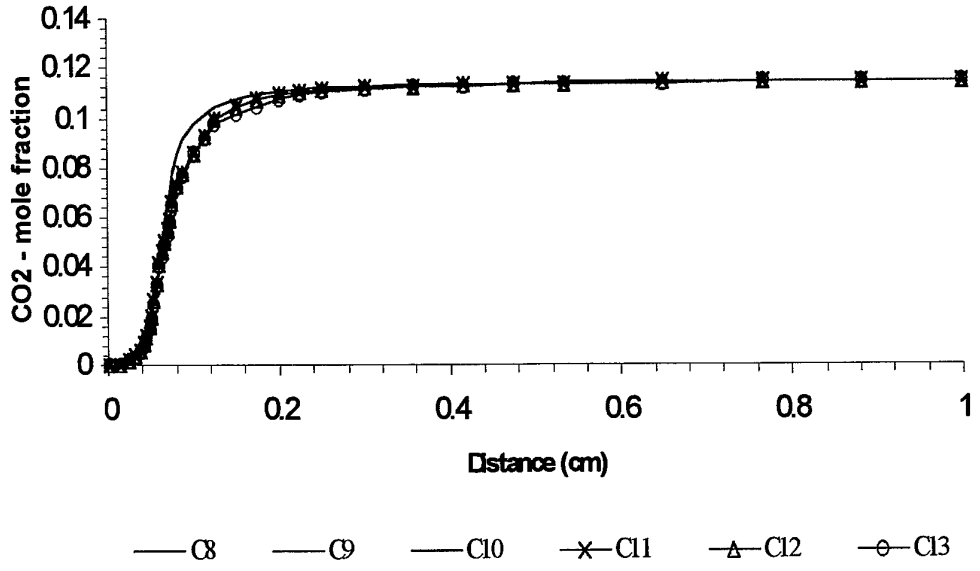

Figure 15: CO_2 mole fraction profiles for configurations C8-1C13 as listed in Tables 2.

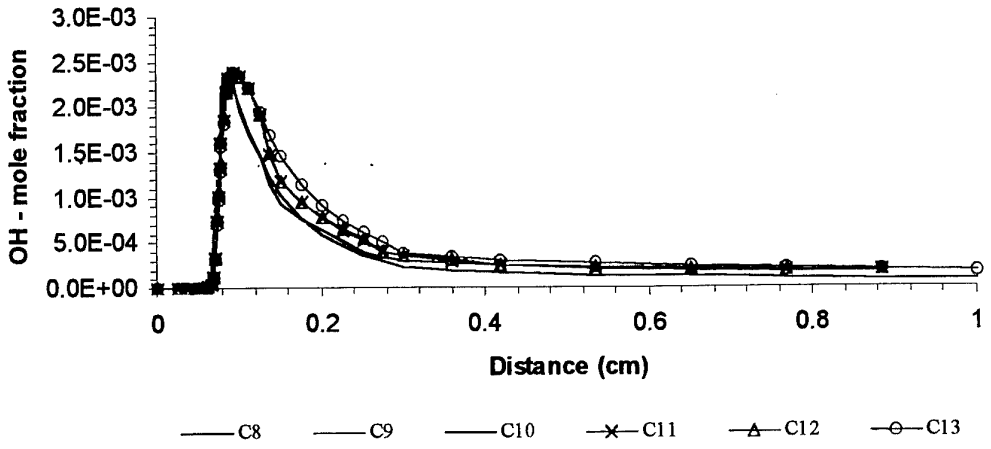

Figure 16: OH mole fraction profiles for configurations C8-1C13 as listed in Tables 2.

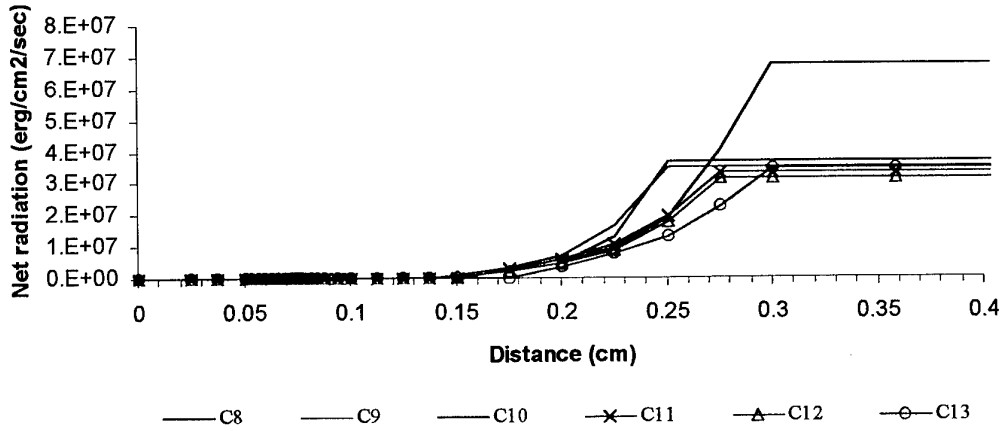

Figure 17: Net radiation for configurations C8-C13, as listed in Table 2.

Comparing configurations C10 and C11, shows that a reduction in the scattering albedo by a factor of nine does not seem to a have significant effect on temperatures or concentrations of major species. The net radiation, however, is reduced by approximately 10%. Configurations C12 and C13 examine the effect of changing the ratio between the forward and backward radiation scattering fractions. By changing the ratio from 1:9 to 8:2 (and even to 1:1 as in most configurations), the only evident effect is a slight reduction in the net radiation of less than 5%.

To summarise, the results of the systematic sensitivity analysis presented above show that out of the nine parameters examined four can be considered influential. These are, in order of significance, the area density, void, reflectivity and the ratio of the forward-

to-backward scattering fractions. The degree to which these parameters affect the results, however, is also influenced by the thickness of the porous layer and by catalytic surface reactions (which have not been included in this study). Therefore, it is essential to recognise that this sensitivity analysis is used in the numerical sense to estimate the effect of variations in input parameters on the solution. This does not necessarily reflect actual physical conditions. That is, in reality there is an inherent coupling between various optical properties, which implies that it is not always possible to alter one parameter while keeping the other unchanged. Fu *et al* [21], for example showed that for cellular ceramic the single scattering albedo increases with the porosity. They also showed that an increase in the material reflectivity leads to an increase in the scattering albedo. Therefore, care should be exercised when assigning optical properties in the model to predict the combustion and radiative performance of actual porous materials.

6. Concluding Remarks

A one-dimensional numerical model, *ChemRad,* for predicting combustion and heat transfer characteristics in porous media has been introduced. The model accounts for detailed chemical kinetics and uses a two-flux radiation model in the energy equation. The capabilities of the model to incorporate detailed gas and surface chemistry schemes, handle multiple layers of different porous materials, and couple the chemistry-radiation provide a flexible tool that can be used to optimise the performance of porous radiant burners.

The main source for potential inaccuracies in the numerical solution arises from uncertainties in the values of certain material properties, the greatest being the optical and the microstructural properties of the porous medium. A sensitivity analysis has been performed to quantify the extent of the solution's sensitivity to nine input parameters. It has been found that the most influential input parameters in order of significance, are the area density, voidage and reflectivity of the porous material, and the ratio between the forward- and backward scattering of radiation.

The robustness of the *ChemRad* model has been successfully demonstrated in a separate study[5], in which numerical predictions have been compared favourably with experimental results.

7. Acknowledgment

Special thanks to Prof. Brian Haynes from the University of Sydney for his valuable comments and discussions.

8. References

1. Williams, A., Woolley, R., and Lawes, M.," The formation of NO_x in Surface Burners", *Combust. Flame* 89:157-166 (1992).

2. Al-Halbouni, A., Sontag R., Giese, R., and Kaferstein, P., "Investigation of NO- and CO-Formation on a Surface Radiant Burner by Considering the Operational Parameters", *Proc. First European Conference on Small Burner Technology and Heating Equipment*, Vol. 1, pp. 75-84, Zurich, September 25-26, 1996.

3. Pulles, C.J.A., "Design of low-NO_x atmospheric Burner for an instantaneous Water Heater", *Proc. First European Conference on Small Burner Technology and Heating Equipment*, Vol. 1, pp. 261-266, Zurich, September 25-26, 1996.

4. Trimis, D. and Durst, F., "Compact low Emission Combustion Reactors with Integrated Heat Exchanger Using Porous Medium Combustion", *Proc. First European Conference on Small Burner Technology and Heating Equipment*, Vol. 1, pp. 109-118, Zurich, September 25-26, 1996.

5. Christo, F. C. and Krishnamoorthy, Lakshmanan , "Experimental and Numerical Analysis of Thermal Radiation of a Porous Radiant Burner", DSTO – Technical Report (*in press*).

6. Bouma, P.H., and Goey, L.P.H., " The Stability of Flames on a Ceramic Foam Surface Burner", *Proc. First European Conference on Small Burner Technology and Heating Equipment*, Vol. 1, pp. 309-318, Zurich, September 25-26, 1996.

7. Goey, L.P.H., Van de Ven, C.H.J., Bouma P.H., and Drift, A.V.D.," Design of Burner for Combustion in Ceramic Foam", *Proc. First European Conference on Small Burner Technology and Heating Equipment*, Vol. 1, pp. 99-108, Zurich, September 25-26, 1996.

8. Moreno, F.E., Pam, R.L. and Chirolo, D.S.," Theory and Application of Ultra Low NO_x Radiant Combustion: Sub 9 PPM Without SCR", *The 1992 International Gas Research Conference*, pp. 402-412.

9. Rumminger, M.D., Dibble, R.W., Heberle, N.H., and Crosley, D.R., "Gas temperature above a porous radiant burner: comparison of measurements and model predictions", *26th Symp. (International) on Combustion*, The Combustion Institute, Pittsburgh, pp. 1755-1762, 1996.

10. Rumminger, M.D., Hamlin, R.D., and Dibble, R.W., "Numerical analysis of a catalytic radiant burner: effect of catalyst on radiant efficiency and operability", Catalysis Today, 1999, 47:253-262,

11. Shardlow, P.J., " A One Dimensional Model for Catalysed Combustion in a Porous Burner", Master of Engineering Research Dissertation, University of Sydney, 1999.

12. Kee, R.J., Rupley, F.M. and Miller, J.A., "CHEMKIN II: A Fortran Chemical Kinetics Package for the Analysis of Gas-Phase Chemical Kinetics", Report SAND 89-8009, Sandia National Laboratories, CA; 1989

13. Coltrin, M.E., Kee, R.J., and Rupley, F.M., " SURFACE CHEMKIN: a Fortran package for analysing heterogeneous chemical kinetics at a solid-surface - gas-phase interface", Report SAND90-8003B, Sandia National Laboratories, CA; 1991.

14. Kee, R.J., Grcar, J.F., Smooke, M.D. and Miller, J.A., A Fortran Computer Program for Modeling Steady Laminar One-Dimensional Premixed Flames, Report SAND 85-8240, Sandia National Laboratories, CA; 1985.

15. Kee, R.J., Dixon-Lewis, G., Warnatz, J. and Miller, J.A., (1986), A Fortran Computer Code Package for the Evaluation of Gas-Phase Multicomponent Transport Properties, Report SAND 86-8246, Sandia National Laboratories, CA.

16. McBride, B. J., "Database of Coefficients for Calculating Thermodynamic and Transport Properties", NASA TM-4513 (1993).

17. Burcat, A., and McBride, B. "1997 Ideal Thermodynamics Data for Combustion and Air-Pollution Use", Technion Aerospace Report TAE804 (June 1997): *ftp://ftp.technion.ae.il/pub/supported/aetdd/thermodynamics*

18. NIST - Species Data http://www.cstl.nist.gov/div386/ckmech/SpeciesData.html

19. Golombok, M., Jariwala, H., and Shirvill, L.C., "Gas-solid heat exchange in a fibrous metallic material measured by a heat regenerator technique", *International Journal of Heat and Mass Transfer,* 33(2):2430252, 1990.

20. GRI-Mech 2.1, "An optimised detailed chemical reactions mechanism for natural gas flames and ignition", http://euler.Berkely.EDU/gri-mech

21. Fu, X., Viskanta, R., and Gore, J.P., "A Model for the Volumetric Radiation Characteristics of Cellular Ceramics", *Int. Comm. Heat Mass Transfer,* Vol. 24, pp. 1069-1082, 1997.

Appendix A: Chemical Kinetics Mechanism

A high temperature kinetics mechanism for propane reactions. The mechanism includes also N-O reactions from the GRI-2.1 mechanism.

SPECIES

CH4 O2 H2O CO2 H O OH HO2 H2 CO H2O2 HCO CH2O CH3 CH3O CH C3H8 N*C3H7 I*C3H7 C3H6 C2H6 C2H5 CH3HCO C2H4 C2H3 CH2CO C2H2 HCCO C2H CH2 N NNH N2 NO NO2 N2O HNO HCNO NH NH2

REACTIONS	(K = A*T^b Exp(-E/RT) A(mole-cm-sec-K)	b	E (cal/mole)
O2 + H=OH + O	1.200E17	-0.91	16530.
H2 + O=OH + H	1.5E7	2.0	7560.
H2 + OH=H2O + H	1.000E08	1.6	3300.
OH + OH=H2O + O	1.500E09	1.14	100.
H +O2 + M = HO2 + M	2.00E18	-0.8	0.
H2O/18.6/ CO2/4.2/ H2/2.86/ CO/2.11/ O2/0.0/ N2/1.26/			
HO2 +H=OH +OH	1.500E14	0.0	1000.
HO2 +H=H2 +O2	2.500E13	0.0	690.
HO2 +H=H2O +O	3.000E13	0.0	1720.
HO2 +OH=H2O +O2	2.000E13	0.0	0.0
CO +OH=CO2 +H	4.400E06	1.5	-740.
CH4 + H = H2 + CH3	2.200E04	3.0	8760.
CH4 + OH = H2O + CH3	1.600E06	2.1	2460.
CH3 + O = CH2O + H	7.000E13	0.	0.
CH3 + OH = CH2O + H + H	4.500E14	0.	15500.
CH3 + OH = CH2O + H2	8.000E12	0.	0.
CH3 + H = CH4	1.9E36	-7.0	9066.
CH2O +H=HCO +H2	2.500E13	0.	4000.
CH2O +OH = HCO +H2O	3.000E13	0.	1200.
HCO + H = CO + H2	2.0E14	0.	0.
HCO + OH = CO + H2O	1.0E14	0.	0.
HCO +O2= CO +HO2	3.000E12	0.	0.
HCO +M = CO+H+M	7.100E14	0.	16820.
CH3 + CH3 = C2H6	1.0E38	-7.66	9500.
C2H6 + H = H2 + C2H5	5.400E02	3.5	5215.
C2H6 + OH = H2O + C2H5	6.300E06	2.0	645.
C2H5 = C2H4 + H	1.0E38	-7.71	49000.
C2H5 + H = CH3 + CH3	3.000E13	0.	0.
C2H5 + O2 = HO2 + C2H4	2.000E12	0.	5000.
C2H4 + OH = C2H3 + H2O	7.000E13	0.	3000.
C2H3 = C2H2 + H	1.600E32	-5.5	46290.
C2H3 + O2 = CH2O + HCO	1.500E12	0.	0.

REACTIONS	(K = A*T^b Exp(-E/RT) A(mole-cm-sec-K)	b	E (cal/mole)
C2H3 + O = CH2CO + H	3.000E13	0.	0.
CH2CO + H = CH3 + CO	7.000E12	0.	3000.
CH2CO + OH =CH2O + HCO	1.000E13	0.	0.
C2H2 + O = HCCO + H	4.300E14	0.	12130.
C2H2 + O = CH2 + CO	4.100E08	1.5	1700.
C2H2 + OH = H2O + C2H	1.000E13	0.	7000.
HCCO + H = CH2 + CO	3.000E13	0.	0.
HCCO + O = CO + CO +H	1.000E14	0.	0.
CH2 +O2 = CO2 +H +H	6.500E12	0.	1500.
CH2 +O2 = CO +OH +H	6.500E12	0.	1500.
CH2 +H=CH +H2	4.000E13	0.	0.
CH +O2 = HCO +O	3.000E13	0.	0.
C2H + O2 = HCCO + O	5.000E13	0.	1500.
C2H + H2 = C2H2 + H	1.100E13	0.	2870.
CH3 + H = CH2 + H2	1.800E14	0.	15070.
CH3 + OH = CH2 + H2O	1.5E13	0.	5000.
CH2 + OH = CH2O + H	2.5E13	0.	0.
CH2 + OH = CH + H2O	4.5E13	0.	3000.
CH + OH = HCO + H	3.0E13	0.	0.
C3H8 + H = N*C3H7 + H2	1.300E14	0.	9710.
C3H8 + OH = N*C3H7 + H2O	3.7E12	0.	1650.
C3H8 + H = I*C3H7 + H2	1.000E14	0.	8350.
C3H8 + OH = I*C3H7 + H2O	2.8E12	0.	860.
N*C3H7 + H = C3H8	2.000E13	0.	0.
I*C3H7 + H = C3H8	2.000E13	0.	0.
N*C3H7 = C2H4 + CH3	3.000E14	0.	33033.
N*C3H7 = C3H6 + H	1.000E14	0.	37340.
N*C3H7 + O2 = C3H6 + HO2	1.000E12	0.	5000.
I*C3H7 = C3H6 + H	2.000E14	0.	38730.
I*C3H7 + O2= C3H6 + HO2	1.000E12	0.	2990.
C3H6 + OH = CH3HCO + CH3	1.0E13	0.	0.
C3H6 + O = C2H5 + HCO	6.8E04	2.6	-1124.
CH3HCO + H = CH3 + CO + H2	4.0E13	0.	4210.
CH3HCO + OH = CH3 + CO + H2O	1.0E13	0.	0.!
N+NO=N2+O	3.500E+13	0.	330.00
N+O2=NO+O	2.650E+12	0.	6400.00
N+OH=NO+H	7.333E+13	0.	1120.00
N2O+O=N2+O2	1.400E+12	0.	10810.00
N2O+O=2NO	2.900E+13	0.	23150.00
N2O+H=N2+OH	4.400E+14	0.	18880.00
N2O+OH=N2+HO2	2.000E+12	0.	21060.00
N2O(+M)=N2+O(+M)	1.300E+11	0.	59620.00
LOW / 6.200E+14 .000 56100.00/			
H2/2.00/ H2O/6.00/ CH4/2.00/ CO/1.50/ CO2/2.00/ C2H6/3.00/			
HO2+NO=NO2+OH	2.110E+12	0.	-480.00
NO+O+M=NO2+M	1.060E+20	-1.410	.00
H2/2.00/ H2O/6.00/ CH4/2.00/ CO/1.50/ CO2/2.00/ C2H6/3.00/			
NO2+O=NO+O2	3.900E+12	0.	-240.00
NO2+H=NO+OH	1.320E+14	0.	360.00

DISTRIBUTION LIST

A Parametric Analysis of a Coupled Chemistry-Radiation Model in Porous Media

Farid C. Christo

AUSTRALIA

DEFENCE ORGANISATION

Task Sponsor **DGAD**

S&T Program

Chief Defence Scientist
FAS Science Policy } shared copy
AS Science Corporate Management
Director General Science Policy Development
Counsellor Defence Science, London (Doc Data Sheet)
Counsellor Defence Science, Washington (Doc Data Sheet)
Scientific Adviser to MRDC Thailand (Doc Data Sheet)
Scientific Adviser Policy and Command
Navy Scientific Adviser (Doc Data Sheet and distribution list only)
Scientific Adviser - Army (Doc Data Sheet and distribution list only)
Air Force Scientific Adviser
Director Trials

Aeronautical and Maritime Research Laboratory
Director

Chief of Weapons Systems Division
Research Leaders (WSD), RLAWS, and RLJI
Head Pyrotechnics, WSD
Head Terminal Effects, WSD
Head Propulsion Systems Technology, WSD
Dr. L. Krishnamoorthy, WSD
Dr. F. Christo, WSD
Dr. N. Smith, AED

DSTO Library and Archives
Library Fishermans Bend (Doc Data Sheet)
Library Maribyrnong (Doc Data Sheet)
Library Salisbury (1 copy)
Australian Archives
Library, MOD, Pyrmont (Doc Data sheet only)

US Defense Technical Information Center, 2 copies
UK Defence Research Information Centre, 2 copies
Canada Defence Scientific Information Service, 1 copy
NZ Defence Information Centre, 1 copy
National Library of Australia, 1 copy

Capability Systems Staff

Director General Maritime Development (Doc Data Sheet only)
Director General Land Development
Director General C3I Development (Doc Data Sheet only)
Director General Aerospace Development (Doc Data Sheet only)

Army

ASNSO ABCA, Puckapunyal, (4 copies)
SO (Science), DJFHQ(L), MILPO Enoggera, Queensland 4051 (Doc Data Sheet only)

Air Force

DDEW
Pyrotechnics and countermeasures Group, JALO, Defence Establishment Orchard Hills, NSW

Intelligence Program

DGSTA Defence Intelligence Organisation
Manager, Information Centre, Defence Intelligence Organisation

Corporate Support Program

Library Manager, DLS-Canberra (Doc Data Sheet only)

UNIVERSITIES AND COLLEGES

Australian Defence Force Academy
Library
Head of Aerospace and Mechanical Engineering
Serials Section (M list), Deakin University Library, Geelong, 3217
Hargrave Library, Monash University (Doc Data Sheet only)
Librarian, Flinders University

OTHER ORGANISATIONS

NASA (Canberra)
AusInfo

OUTSIDE AUSTRALIA

ABSTRACTING AND INFORMATION ORGANISATIONS

Library, Chemical Abstracts Reference Service
Engineering Societies Library, US
Materials Information, Cambridge Scientific Abstracts, US
Documents Librarian, The Center for Research Libraries, US

INFORMATION EXCHANGE AGREEMENT PARTNERS

Acquisitions Unit, Science Reference and Information Service, UK
Library - Exchange Desk, National Institute of Standards and Technology, US
National Aerospace Laboratory, Japan
National Aerospace Laboratory, Netherlands

SPARES (5 copies)

Total number of copies: **52**

DEFENCE SCIENCE AND TECHNOLOGY ORGANISATION
DOCUMENT CONTROL DATA

1. PRIVACY MARKING/CAVEAT (OF DOCUMENT)

2. TITLE

A Parametric Analysis of a Coupled Chemistry-Radiation Model in Porous Media

3. SECURITY CLASSIFICATION (FOR UNCLASSIFIED REPORTS THAT ARE LIMITED RELEASE USE (L) NEXT TO DOCUMENT CLASSIFICATION)

Document	(U)
Title	(U)
Abstract	(U)

4. AUTHOR(S)

Farid C. Christo

5. CORPORATE AUTHOR

Aeronautical and Maritime Research Laboratory
PO Box 4331
Melbourne Vic 3001 Australia

6a. DSTO NUMBER	6b. AR NUMBER	6c. TYPE OF REPORT	7. DOCUMENT DATE
DSTO-RR-0188	AR-011-608	Research Report	October 2000

8. FILE NUMBER	9. TASK NUMBER	10. TASK SPONSOR	11. NO. OF PAGES	12. NO. OF REFERENCES
J-9505-19-53-1	97/250	DGAD	27	21

13. URL ON THE WORLD WIDE WEB

http://www.dsto.defence.gov.au/corporate/reports/DSTO-RR-0188.pdf

14. RELEASE AUTHORITY

Chief, Weapons Systems Division

15. SECONDARY RELEASE STATEMENT OF THIS DOCUMENT

Approved for public release

OVERSEAS ENQUIRIES OUTSIDE STATED LIMITATIONS SHOULD BE REFERRED THROUGH DOCUMENT EXCHANGE, PO BOX 1500, SALISBURY, SA 5108

16. DELIBERATE ANNOUNCEMENT

No Limitations

17. CASUAL ANNOUNCEMENT Yes

18. DEFTEST DESCRIPTORS

Pyrotechnics, combustion, modelling, chemical kinetics, porous media, infrared

19. ABSTRACT

A one-dimensional coupled chemistry-radiation model (ChemRad) for predicting combustion and heat transfer characteristics in a single and multi-layered porous media is presented. The model allows detailed gas and surface chemical kinetics mechanisms to be incorporated, and uses a two-flux radiation approximation in the energy equation. A stoichiometric propane/air mixture burning in a thin wire-mesh burner has been modelled using a well-documented high-temperature propane kinetics scheme with 40 reactive species and 93 reactions. A systematic analysis of the solution's sensitivity to variations in input parameters, particularly the optical characteristics of the media, has been performed and influential parameters have been identified. It has been found that the dominant factors that influence the solution, in order of significance are the area density, voidage and reflectivity of the porous material, and the ratio of forward-to-backward scattering of radiation.